

Supplemental Material for:

Dancing Ejecta

Y. S. Tian*,^{1,2} A. B. Aljedaani*,^{1,3} Tariq Alghamdi,^{1,4} and S. T. Thoroddsen¹

¹*Division of Physical Sciences and Engineering, King Abdullah University of Science and Technology (KAUST), Thuwal 23955-6900, Saudi Arabia**

²*School of Construction Machinery, Chang'an University, Xi'an 710064, China*

³*KAUST Upstream Research Center (KURC), EXPEC Advanced Research Center, Saudi Aramco Thuwal 23955-6900, Kingdom of Saudi Arabia*

⁴*Mechanical Engineering Department, College of Engineering and Islamic Architecture, Umm Al-Qura University, Makkah, Saudi Arabia*

A. Different Glycerol/Water mixtures

The viscosities of the drop and the film were changed using different mixtures of water and glycerin. Table S0 lists the various physical properties of these mixtures vs the weight fraction of the glycerin.

B. Ejecta Stretching

To study the in-plane stretching of the ejecta we discretized the arclength of ejecta shapes from the parametric equations of the ballistic ejecta model from Thoroddsen *et al.* [1], after normalizing lengths with R_{sp} and time by R_{sp}/V_{sp} :

$$x(t, \tau) = \sqrt{t(2-t)} + C(1-t)^2(\tau-t); \quad y(t, \tau) = C(1-t)\sqrt{t(2-t)}(\tau-t), \quad (1)$$

which shows the ejecta shape at time τ and the time of ejection $t \leq \tau$ is the parameter along the sheet. The model consists of a sphere penetrating through the pool surface without deforming it, with the ejecta emerging from the contact point

$$x_c(t) = \sqrt{V_{sp}t(2R_{sp} - V_{sp}t)},$$

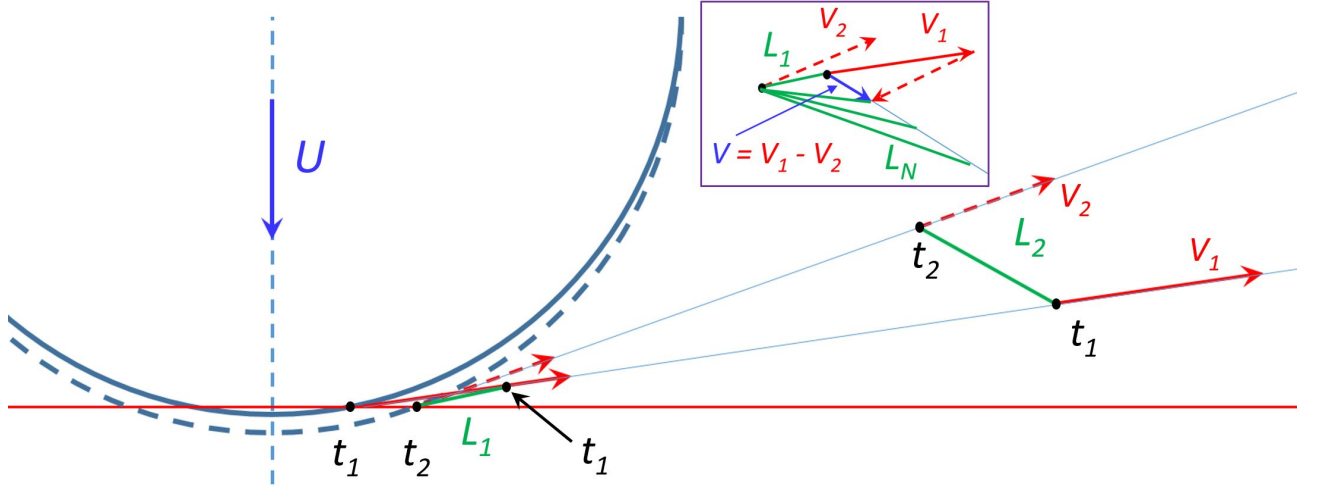
when its radial velocity becomes smaller than the ejecta

$$V_c = \frac{dx_c}{dt} = \frac{V_{sp}(R_{sp} - V_{sp}t)}{\sqrt{V_{sp}t(2R_{sp} - V_{sp}t)}} \leq C V_{sp} \cos\theta.$$

TABLE S0. Density (ρ), Viscosity (μ) and surface tension (σ) of Glycerin/Water weight mixtures at $T = 23^\circ$.

$w_{Glycerol}$ %	ρ [kg/m ³]	μ [cP]	σ [mN/m]
70	1179	19.8	66.2
80	1206	50.9	65.3
83.9	1217	79.4	64.9
85.4	1221	96.3	64.8
88.3	1228	141	64.5
91.6	1237	231	64.2
93	1241	289	64.1
94.9	1246	397	63.9
97.9	1254	697	63.6
100	1261	1078	63.4

* These authors contributed equally.



Supplemental Figure S1. The overall stretching and rotation of a typical element of the ejecta. The inset shows the stretching in the coordinates moving with point of the sheet ejected at $t = t_2$.

Early on $\cos\theta \simeq 1$ and the equality becomes

$$C^2 V_{sp} t (2R_{sp} - V_{sp} t) = C^2 [2R_{sp} V_{sp} t - V_{sp}^2 t^2] = R_{sp}^2 - 2R_{sp} V_{sp} t + V_{sp}^2 t^2$$

for small time the sphere has only penetrated a small distance, thereby $V_{sp} t \ll R_{sp}$, giving $t_c \simeq R_{sp} / (2C^2 V_{sp})$.

Figure S1 sketches the in-plane stretching of a short fluid element along the sheet, where the start of the element emerges at t_1 and the end of it is ejected at t_2 . Each end is projected along a straight line at a constant speed. As the ejecta speed is larger at the start, according to the model, the element is stretched in time. Furthermore, the ejecta direction changes, which tends to rotate the element. In the frame of reference of the t_2 end, the inset in Fig. S1 shows how the velocity difference and direction stretches and rotates the sheet element.

C. Ejecta Evolution

We use the local stretching, in terms of an arclength parameter, to distribute the nodal points uniformly along the sheet. To accomplish this we to determine the values of t based on the values of the derivatives of Eq. (1), i.e.

$$\frac{\partial x}{\partial t} = \frac{(1-t)}{\sqrt{t(2-t)}} - C(1-t)[2\tau - 3t + 1]; \quad \frac{\partial y}{\partial t} = C \left[\frac{\tau - 4\tau t + 2\tau t^2 - 3t + 7t^2 - 3t^3}{\sqrt{t(2-t)}} \right].$$

D. Ejecta - Elliptical Kinematic Model

Owing to air resistance the drops are deformed away from spherical, during the free-fall, to become oblate at the impact. We have also built a kinematic model in the vein of [1], now using an elliptic drop: The equation of the ellipse shown in Figure S2 is

$$\frac{x^2}{a^2} + \frac{(y - y_0)^2}{b^2} = 1 \quad (2)$$

where a is the x -radius and b is the y -radius, their aspect ratio is defined as $\beta = b/a$. The y -coordinate of the drop center is a function of time t ,

$$y_0 = b - V_i t \quad (3)$$

The intersection point x_c is calculated combining the formula for the ellipse and x -axis.

$$x_c = \frac{1}{\beta} \sqrt{(2b - V_i t) V_i t} \quad (4)$$

where V_i is the impact velocity of the ellipse.

Note that, the ejection velocity, V_e , is angled with horizontal axis at α , which is not equal to the angle θ . The slope of the ellipse at the intersection point is

$$\frac{dy}{dx} = \frac{\beta x}{\sqrt{1-x^2}}.$$

the trajectory of each fluid element

$$x(\tau, t) = x_c + V_e \cos \alpha (\tau - t); \quad y(\tau, t) = V_e \sin \alpha (\tau - t) \quad (5)$$

where the ejection velocity V_e directed tangentially to the ellipse at the intersection, say the angle is α , is assumed to be proportional to the normal impact velocity,

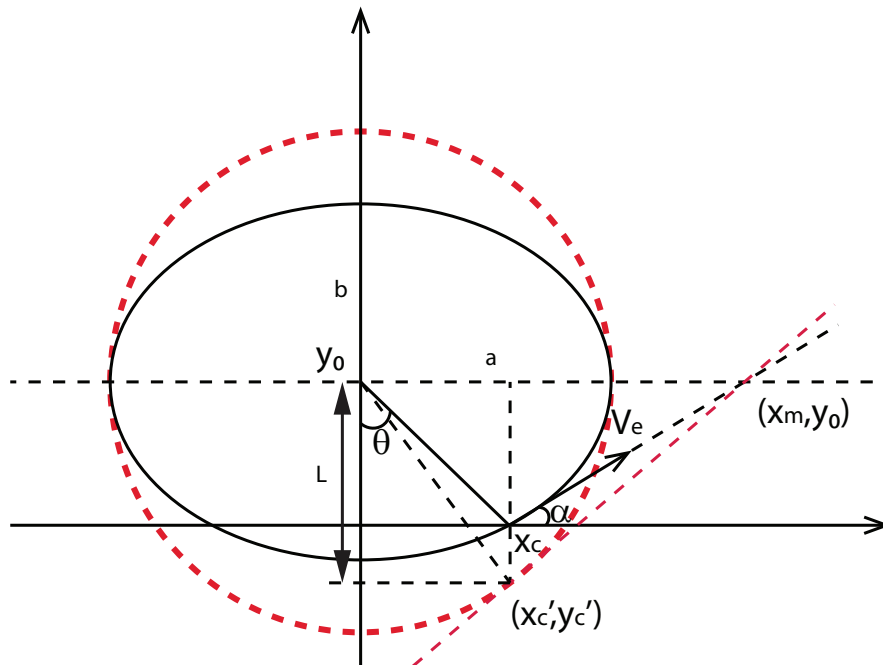
$$V_e = C V_i \cos \alpha \quad (6)$$

where C is the ejecta-speed constant, shown in Fig. 4(a) in the main text. Substitute Equation 6 into 5,

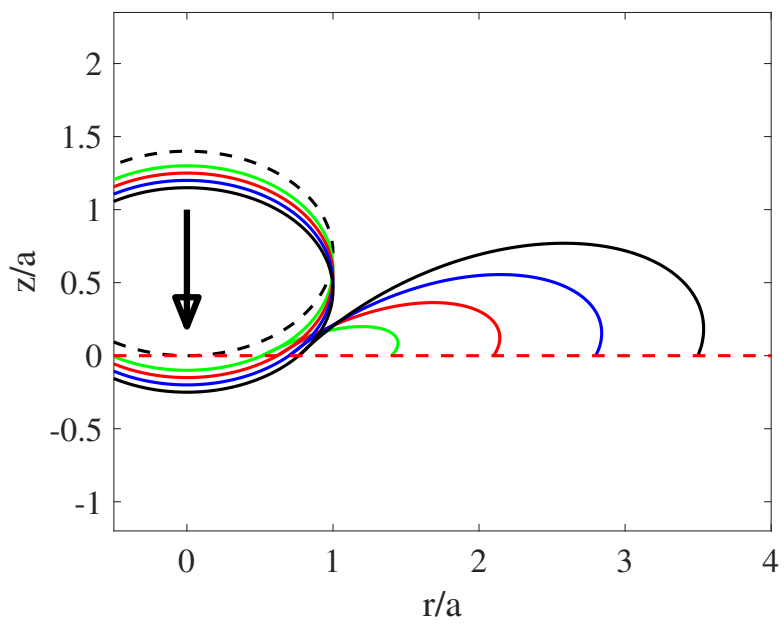
$$x(\tau, t) = x_c + V_i \cos^2 \alpha (\tau - t); \quad y(\tau, t) = V_i \cos \alpha \sin \alpha (\tau - t) \quad (7)$$

Combining these equations we get a formula for the ejecta shapes for an ellipse of aspect ratio β , at time τ :

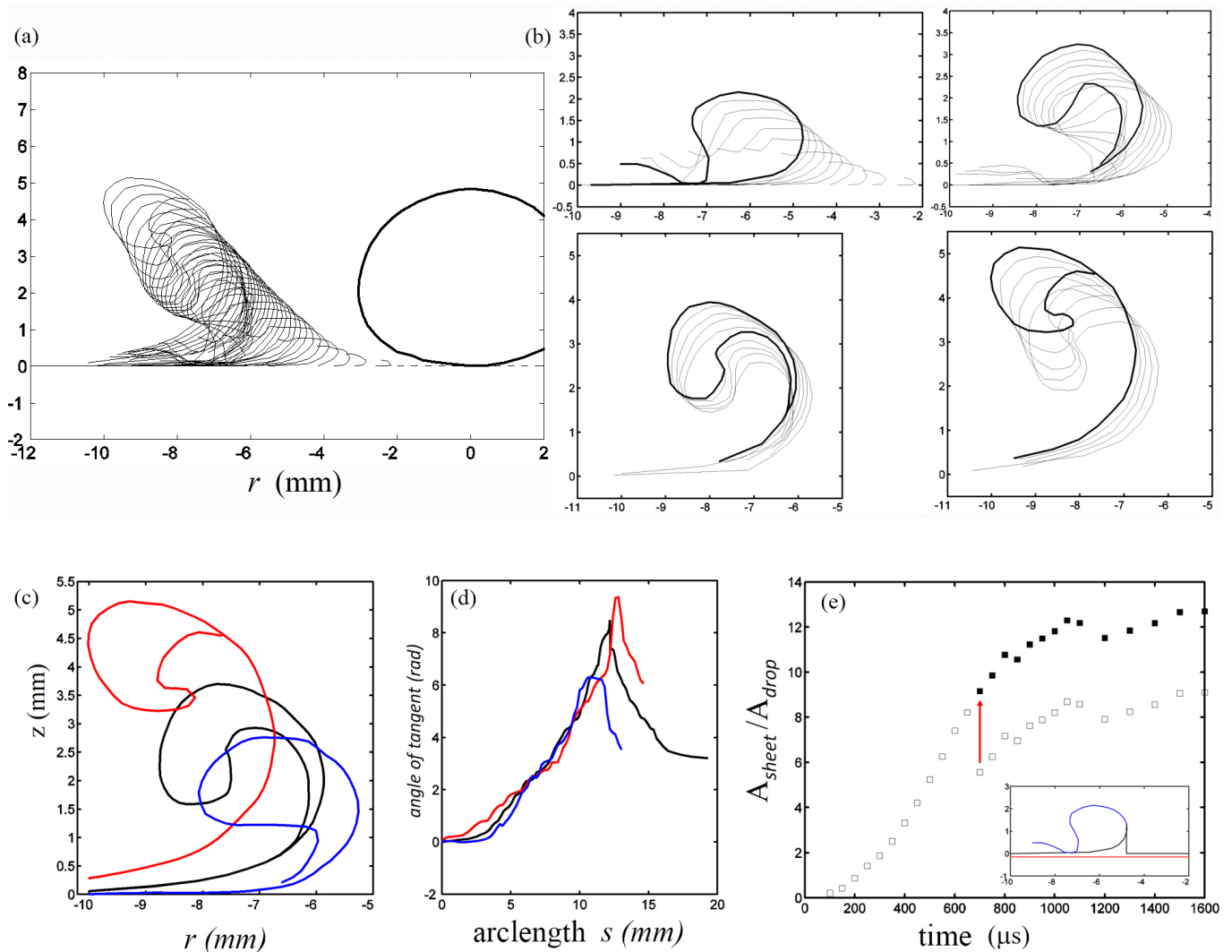
$$x(t, \tau) = \frac{1}{\beta} \sqrt{t(2\beta - t)} + \frac{C(t - \beta)^2(\tau - t)}{\beta^2 + (\beta^2 - 1)t(2\beta - t)}; \quad y(t, \tau) = \frac{C\beta(\beta - t)\sqrt{t(2\beta - t)}(\tau - t)}{\beta^2 + (\beta^2 - 1)t(2\beta - t)}.$$



Supplemental Figure S2. Sketch of the Elliptical Kinematic Model. V_e shows the angle of ejecting velocity, α , which is not the same as θ .



Supplemental Figure S3. The model prediction of the ejected sheets for an impact of an ellipsoidal drop, with aspect ratio $\beta = b/a = 0.70$, shown at $\tau = 0.1, 0.15, 0.2$ & 0.25 for $C = 14$.

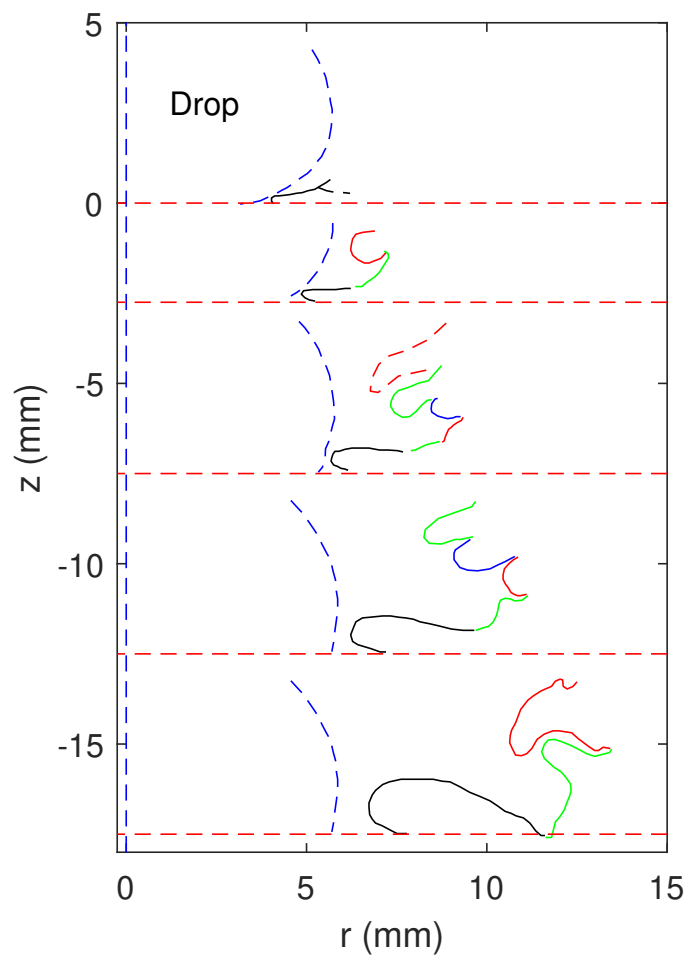


Supplemental Figure S4. (a) Ejecta shape evolution, spaced by $50 \mu\text{s}$, for $Re = 1050$ and $We = 4950$ based on the corresponding spherical drop diameter. (b) To reduced clutter we split the evolution in (a) into four separate plots. (c,d) Three representative shapes, with the rotation of the tangent as one moves along the sheet. (e) The total area of the sheet vs time. The jump corresponds to the rupture and slingshot of the tip section. The solid symbols add this area to the growing area of the intact sheet. See also Supplemental Video SM1.

E. Ejecta Shapes

Figure S5 shows traces of the ejecta shapes from Supplemental Video SM1, for lower impact velocity, taken in our lab with regular ceiling height. The growth rate of the area is much slower than for the higher impact velocity in the main text. Here the sheet area grows by $12 \times A_{\text{drop}}$ in 1 ms, while in Fig. 7 this stretching is about 17 times faster and only takes $\sim 60 \mu\text{s}$.

[1] Thoroddsen, S. T., Thoraval, M.-J., Takehara, K. & Etoh, T. G. Droplet splashing by a slingshot mechanism. *Phys. Rev. Lett.* **106**, 034501 (2011).



Supplemental Figure S5. Ejecta shapes from Figure 8(b) in the main text, now plotted separately to minimize clutter. Ejecta profiles are shown at 11, 19, 31, 42 and 56 μs after first contact of the drop. The colors follow bent segments in time, but disappear when they rupture in to fine spray. The dashed horizontal red lines show the initial surface level of the liquid film. The vertical dashed blue line is the drop axis of symmetry. See also Supplemental Video SM1.